

Global Circulation and Water Properties: Supplementary Materials

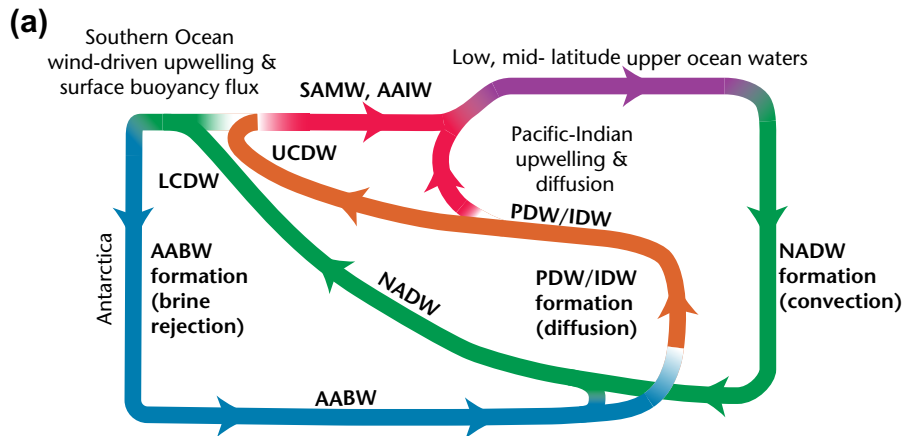


FIGURE S14.1 (a) Two-dimensional schematic of the interconnected NADW, IDW, PDW, and AABW cells of Figure 14.13. (b). Global overturning schematic that mirrors the globally-averaged overturning streamfunction, hence concealing deep upwelling in the Indian and Pacific Oceans. (c) Implied global overturning in the Broecker schematic of Figure 14.12, which ignores the Southern Ocean upwelling and AABW formation. ©American Meteorological Society. Reprinted with permission. *Source: From Talley (submitted, 2011b).*

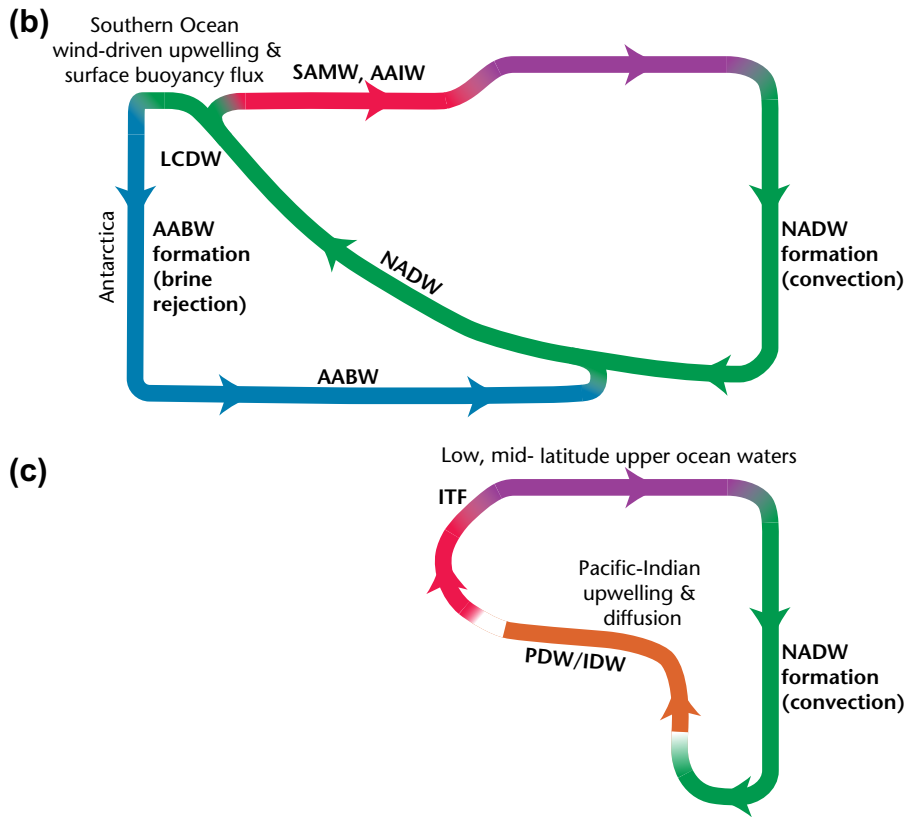


FIGURE S14.1 (Continued).

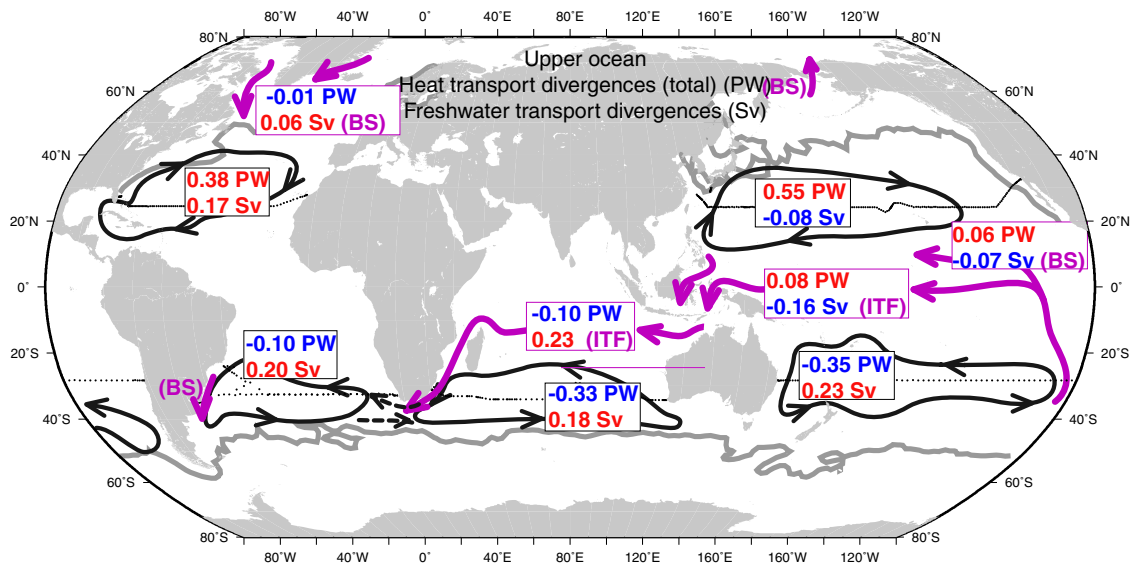


FIGURE S14.2 Estimated mean annual meridional (a) heat transport ($1 \text{ PW} = 10^{15} \text{ W}$) and (b) freshwater transport (Sv) by the subtropical gyres (black contours), resulting from poleward mass transport in the western boundary currents and subducted equatorward return flow, all within and above the main pycnocline. The contributions of the Indonesian Throughflow (magenta contours) and Bering Strait (magenta) are also shown. After Talley (2003, 2008).

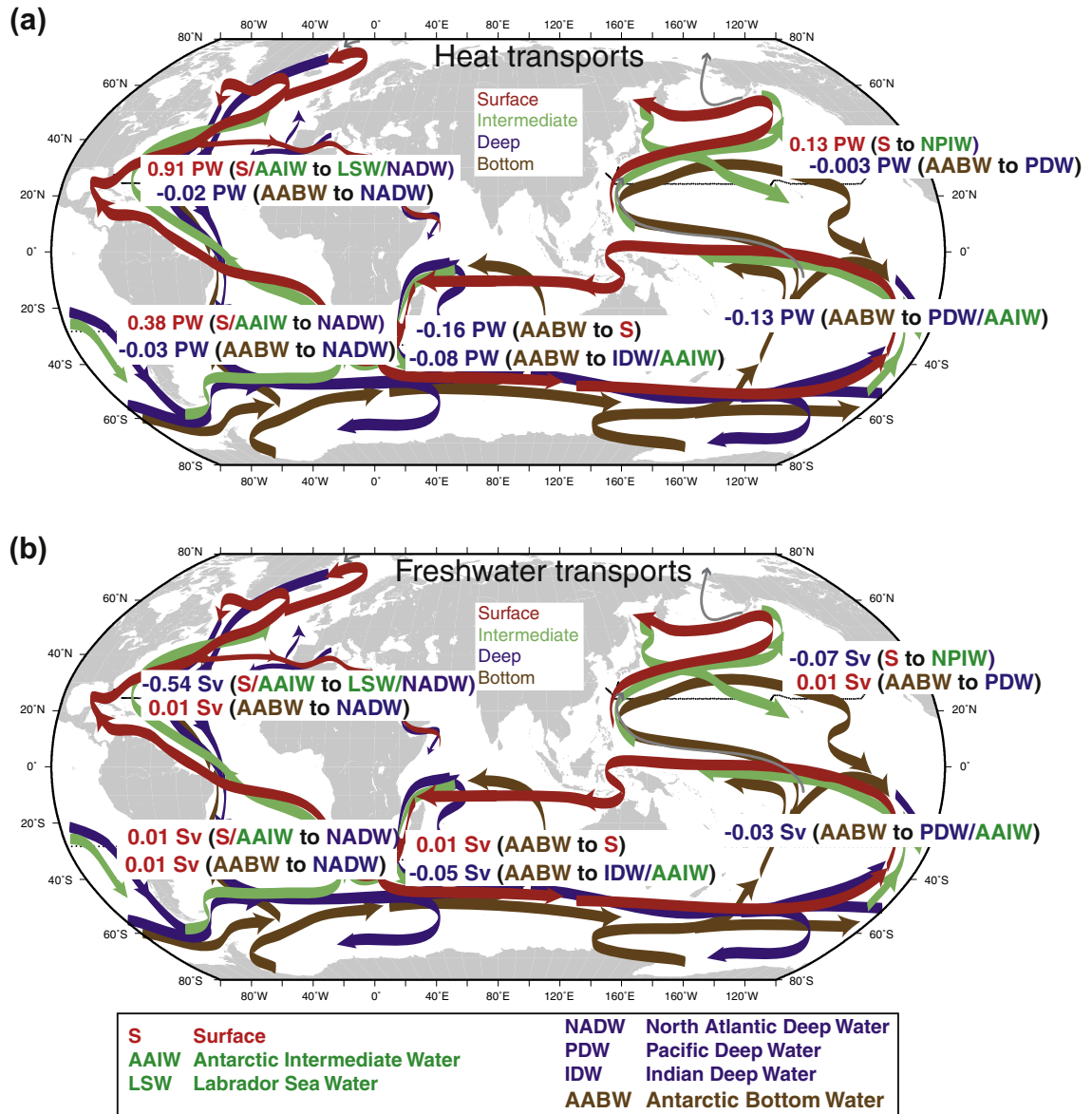


FIGURE S14.3 Estimates of mean annual meridional (a) heat (PW) and (b) freshwater (Sv) transport by elements of the overturning circulation. Acronyms indicate the type of overturn; for instance, AABW to NADW means that the listed transport is associated with overturn of AABW to NADW (upwelling in this instance). *After Talley (2003, 2008).*

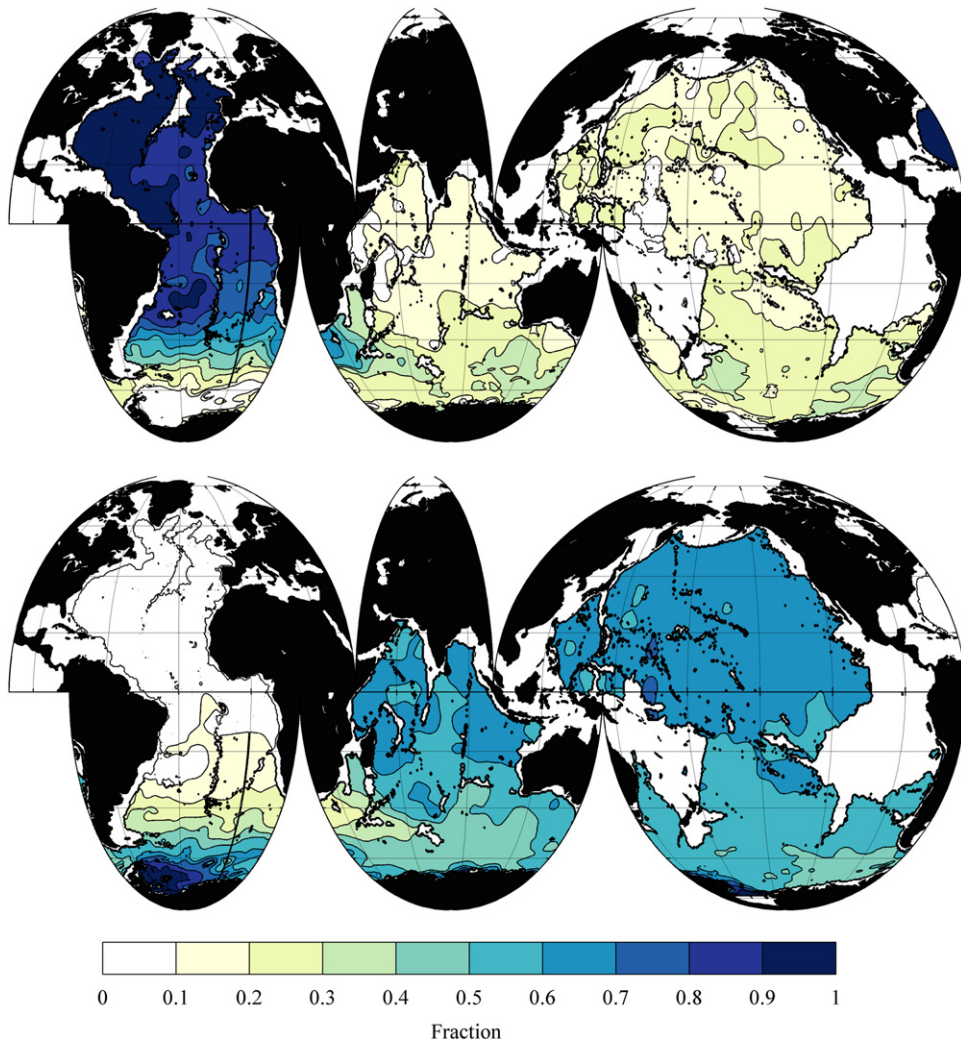


FIGURE S14.4 Fraction of waters on the isoneutral surface $\gamma^N = 28.06 \text{ kg/m}^3$ ($\sigma_4 \sim 45.84 \text{ kg/m}^3$, at a depth of 2500–3000 m north of the ACC) that are (top) North Atlantic Deep Water and (bottom) Antarctic Bottom Water, calculated as in Figure S14.5. *Personal communication, Gregory C. Johnson (2009).*

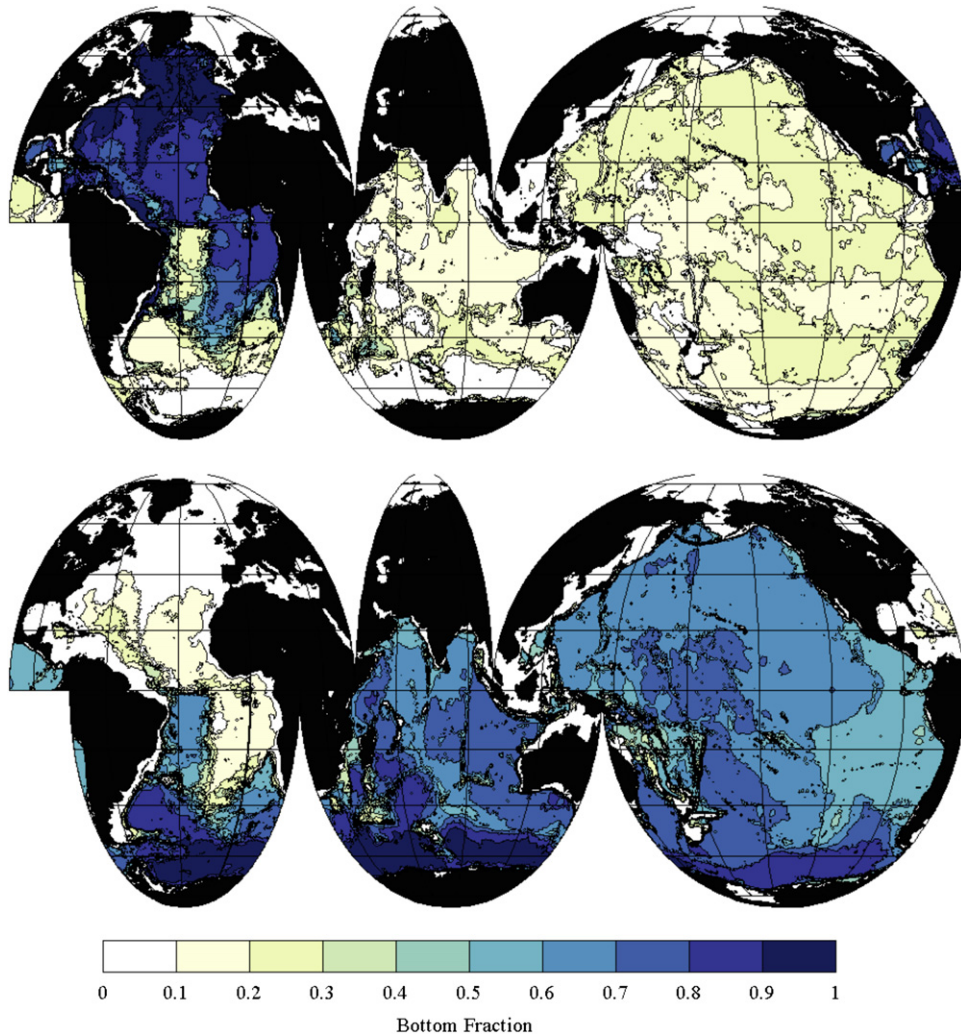


FIGURE S14.5 Fraction of bottom waters that are (top) North Atlantic Deep Water and (bottom) Antarctic Bottom Water, from an optimum multiparameter analysis using as inputs the properties of NADW at a location just south of Greenland, downstream from the Nordic Seas Overflows, and of AABW in the Weddell Sea. *Source: From Johnson (2008).*

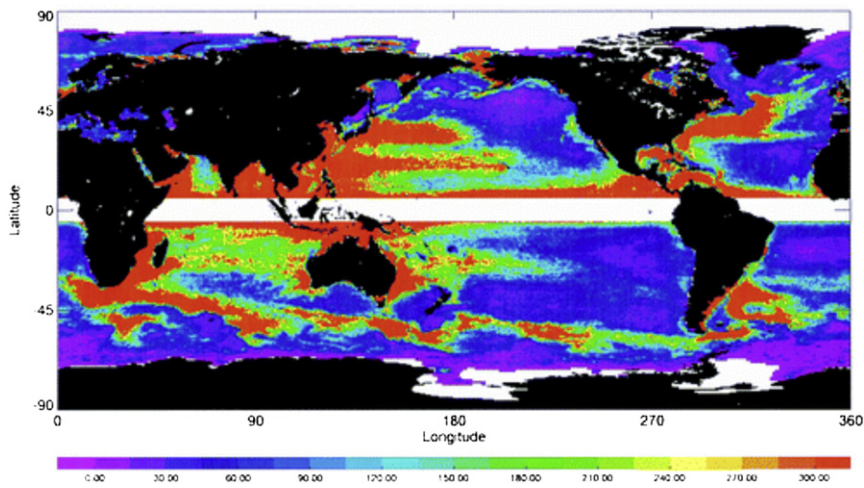


FIGURE S14.6 Eddy kinetic energy from geostrophic velocities calculated from satellite altimetry from 1992 to 1998. The equatorial band is blank because geostrophic velocities cannot be calculated there. This is a companion to Figure 14.16 in the text. *Source: From Ducet, Le Traon, and Reverdin, (2000).*

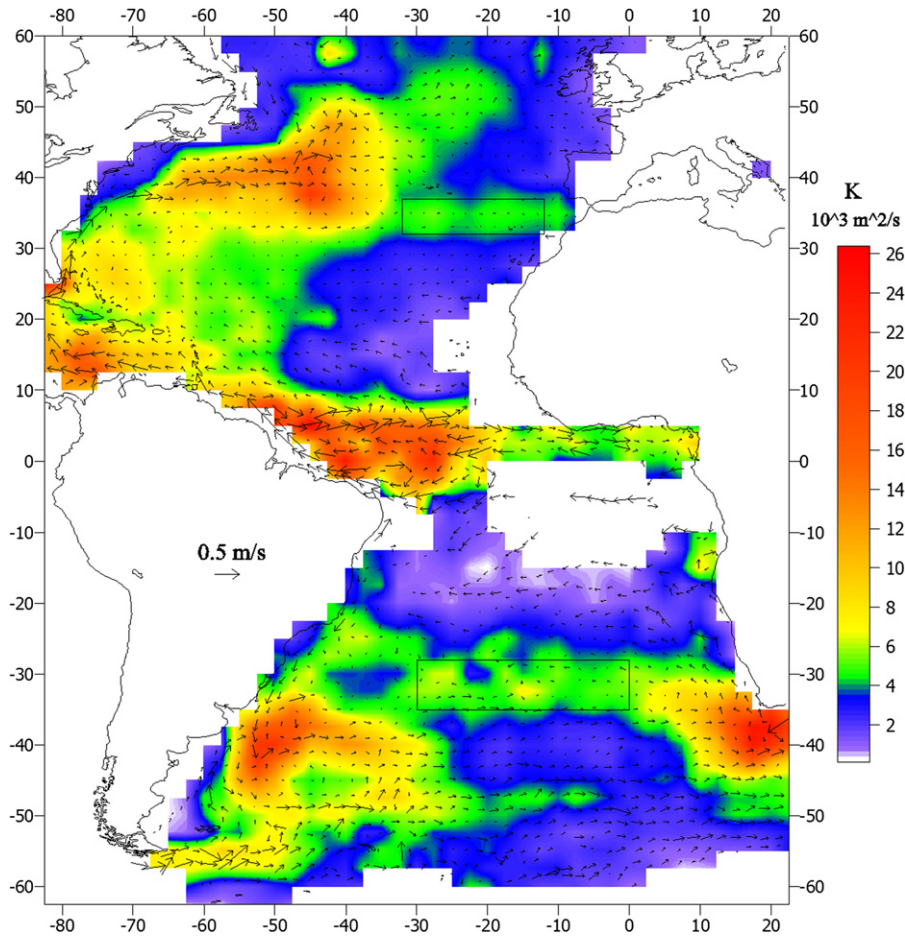


FIGURE S14.7 Horizontal eddy diffusivity (m^2/sec) at the sea surface (color) in the Atlantic Ocean, with mean velocity vectors, based on surface drifter observations. This is a companion to Figure 14.17a. Source: From Zhurbas and Oh (2004).

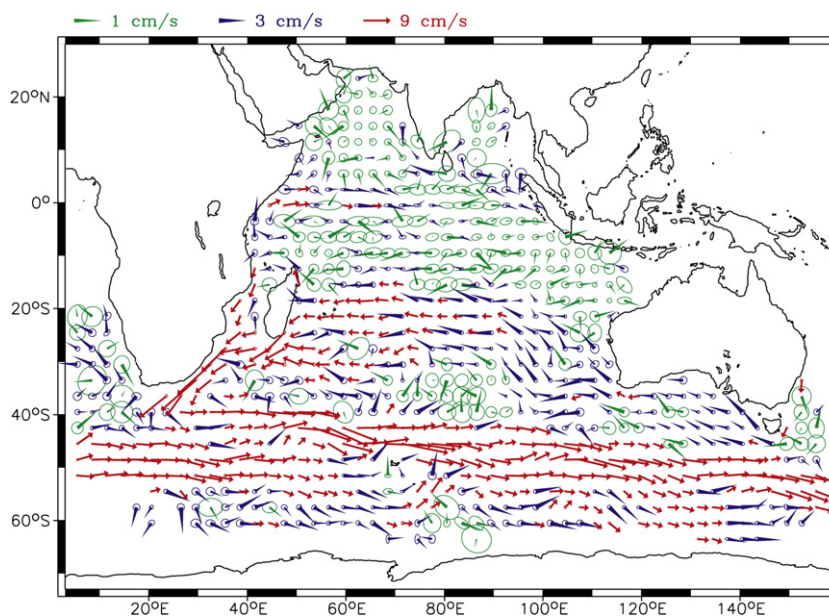


FIGURE S14.8 Eddy diffusivity ellipses at 900 m in the Indian Ocean based on subsurface float velocities. Colors indicate different scales (see figure header). This is a companion to Figure 14.17b. ©American Meteorological Society. Reprinted with permission. Source: From *Davis (2005)*.

References

- Davis, R.E., 2005. Intermediate-depth circulation of the Indian and South Pacific Oceans measured by autonomous floats. *J. Phys. Oceanogr.* 35, 683–707.
- Ducet, N., Le Traon, P.Y., Reverdin, G., 2000. Global high-resolution mapping of ocean circulation from TOPEX/Poseidon and ERS-1 and -2. *J. Geophys. Res.* 105, 19477–19498.
- Johnson, G.C., 2008. Quantifying Antarctic Bottom Water and North Atlantic Deep Water volumes. *J. Geophys. Res.* 113, C05027. doi:10.1029/2007JC004477.
- Talley, L.D., 2003. Shallow, intermediate, and deep overturning components of the global heat budget. *J. Phys. Oceanogr.* 33, 530–560.
- Talley, L.D., 2008. Freshwater transport estimates and the global overturning circulation: Shallow, deep and throughflow components. *Progr. Oceanogr.* 78, 257–303. doi:10.1016/j.pocean.2008.05.001.
- Talley, L.D., 2011b. Schematics of the global overturning circulation. *J. Phys. Oceanogr.*, submitted.
- Zhurbas, V., Oh, I.S., 2004. Drifter-derived maps of lateral diffusivity in the Pacific and Atlantic Oceans in relation to surface circulation patterns. *J. Geophys. Res.* 109, C05015. doi:10.1029/2003JC002241.

